Published in final edited form as:
Biomaterials. 2020 October 01; 255: 120209. doi:10.1016/j.biomaterials.2020.120209.

Targeted nanoparticles towards increased L cell stimulation as a strategy to improve oral peptide delivery in incretin-based diabetes treatment

Yining Xu[1], **Herlinde De Keersmaecker**[2,3], **Kevin Braeckmans**[2,3], **Stefaan De Smedt**[2,3], **Patrice D. Cani**[4], **Véronique Préat**[1], **Ana Beloqui**[1,*]

[1]Université catholique de Louvain, Louvain Drug Research Institute, Advanced Drug Delivery and Biomaterials, 1200 Brussels, Belgium

[2]Ghent University, Faculty of Pharmaceutical Sciences, Laboratory for General Biochemistry and Physical Pharmacy, 9000 Ghent, Belgium

[3]Ghent University, Center for Advanced Light Microscopy, 9000 Ghent, Belgium

[4]Université catholique de Louvain, Louvain Drug Research Institute, Metabolism and Nutrition Research Group, WELBIO (Walloon Excellence in Life sciences and BIOtechnology), 1200 Brussels, Belgium

Abstract

The delivery of therapeutic peptides via the oral route remains one of biggest challenges in the pharmaceutical industry. Recently, we have described an alternative improved drug delivery system for peptide delivery via the oral route, consisting of a lipidic nanocapsule. Despite the striking effects observed, it is still essential to develop strategies to strengthen the nanocarriers' glucagon-like peptide-1 (GLP-1) secretory effect of the nanocarrier and/or prolong its antidiabetic effect *in vivo* to facilitate its translation into the clinic. For this purpose, we developed and compared different fatty acid-targeted lipid and polymeric nanoparticles and evaluated the L cell stimulation induced by the nanocarriers in murine L cells *in vitro* and in normal healthy mice *in vivo*. We further examined the antidiabetic effect *in vivo* in an obese/diabetic mouse model induced by high-fat diet feeding and examined the effect of the oral administration frequency. Among the tested nanocarriers, only lipid-based nanocarriers that were surface-modified with DSPE-PEG_{2000} on the surface were able to significantly strengthen the biological effect of the nanocarriers. They increased endogenous GLP-1 levels up to 8-fold *in vivo* in normoglycemic mice. Moreover, they effectively prolonged the *in vivo* antidiabetic effect by normalizing the plasma glucose levels in obese/diabetic mice following long-term treatment (one month). Ultimately, the targeted nanocarriers were as effective when the administration frequency was reduced from once daily to once every other day.

*Correspondence to: Prof. Ana Beloqui, UCLouvain, Université catholique de Louvain, Louvain Drug Research Institute, Advanced Drug Delivery and Biomaterials, 1200 Brussels, Belgium, Tel +32 (0)27647329. ana.beloqui@uclouvain.be.

Europe PMC Funders Author Manuscripts

Keywords

Targeted nanocarriers; lipid nanocapsules; L cells; type 2 diabetes mellitus; oral peptide delivery; GLP-1

1 Introduction

Therapeutic peptides (more than 60 peptide drugs [1]) are now commercialized via parenteral administration [2]. The delivery of therapeutic peptides via the oral route remains a challenge, especially regarding the low oral bioavailability (less than 1%) of these peptides. Despite these challenges, the advantages of the oral route are remarkable, ameliorating the shortcomings of the parenteral route (e.g., needle phobia, non-patient convenience) [3, 4]. The development of oral delivery systems that allow the absorption of peptides into the systemic circulation is still one of the greatest challenges for the pharmaceutical industry [5]. This is especially true in the treatment of chronic diseases such as type 2 diabetes mellitus (T2DM), where daily injections can be required. T2DM consists of an array of dysfunctions including a marked insulin resistance, characterized by a defect in insulin-mediated glucose uptake in muscle, a disruption of adipocytes function, an impaired insulin action in the liver and eventually a complete dysfunction of the pancreatic β-cells [6]. Glucagon-like peptide-1 (GLP-1) is secreted from enteroendocrine L cells in the gut and has emerged as an antidiabetic peptide due to its multiple physiological effects related to T2DM. GLP-1 promotes insulin secretion and decreases glucagon secretion in the pancreas in a glucose-dependent manner, increasing insulin sensitivity; its effects disappear, reducing the risk of unwanted hypoglycemic events [7]. The oral administration of these gut hormone mimetic peptides could simulate the normal physiological pathway of native incretin peptides [8], which can access the liver in much higher concentrations through the hepatic portal vein, avoiding extensive systemic exposure and its associated side effects [9].

The first GLP-1 analog has reached the market (semaglutide, Rybelsus®, NovoNordisk), representing a major breakthrough in the oral delivery of peptides [10]. The formulation is based on the co-administration of the peptide with a permeation enhancer (sodium N-[8-(2-hydroxybenzoyl) amino] caprylate (SNAC). The formulation presents two main limitations: 1) small differences in the peptide or the SNAC substantially affect the absorption efficacy (variable bioavailability) and 2) according to the authors, the co-administration of SNAC with liraglutide failed to provide circulating levels of liraglutide (the efficacy is limited to the administration of the GLP-1 analog semaglutide (half-life of 165 h)). We have recently described what we believe would represent an alternative improved drug delivery system for the oral delivery of peptides, consisting of a lipid-based nanocapsule [11]. Regardless of the encouraging properties of nanomedicines [11–13], they still must demonstrate superiority to standard formulations incorporating functional excipients in oral peptide delivery [14]. We have developed a dual-action approach that synergizes the biological effect of nanocarriers (inducing endogenous GLP-1 secretion) with that of the encapsulated molecule (increased absorption of the encapsulated peptide). In our proof-of-concept studies, we encapsulated exenatide (half-life of 2.5 h) as a model GLP-1 analog to demonstrate that our strategy we can achieve a therapeutic effect with a short half-life peptide [11]. We conducted a long-term

Europe PMC Funders Author Manuscripts

treatment study (one month) in a chronic model of type 2 diabetes mellitus (T2DM) in mice. Our results demonstrated that this strategy was at least as efficient as the marketed drug (Byetta®, subcutaneous injection) and could even be more potent for improving insulin resistance, oral glucose tolerance and hepatic steatosis. In addition, our approach offers an important advantage over current strategies for oral delivery of incretin mimetic peptides, providing increased endogenous GLP-1 stimulation. These findings allow the potential use of a lower dose in a foreseen application and proven effectiveness with a short half-life peptide, avoiding potential associated toxicity related to the accumulation of a long half-life peptide following daily administrations.

Despite the striking effects observed, it is still essential to develop strategies to strengthen the nanocarrier GLP-1 secretory effect and/or prolong its antidiabetic effect *in vivo* to facilitate its translation into the clinic. We hypothesized that this could be attained by modulating the effect of our lipid-based drug delivery system by tailoring the surface of the nanocarriers.

Enteroendocrine L cells express various G protein-coupled receptors (GPCRs) that are activated by different dietary nutrients present in the lumen to modulate the secretion of hormones (e.g., GLP-1) [15]. Each GPCR has its own ligands, thereby correspondingly modulating the different gut hormones secreted from L cells. For instance, free fatty acid receptors FFAR2 and FFAR3, also known as GPR43 and GPR41, are activated by short-chain fatty acids (SCFAs) (e.g., acetate, propionate, butyrate), stimulating GLP-1 secretion [16]. SCFA propionate displays similar agonism both on FFAR2 and FFAR3, whereas acetate and butyrate only have high affinity for FFAR2 and FFAR3, respectively [17, 18]. In addition, propionate is an end-product of fermentation and thus is not cross-metabolized by the microbiota, unlike acetate and butyrate [19]. We hypothesized that grafting propionate on the surface of our lipid-based nanosystem could lead to an increased GLP-1 secretory effect by directly targeting L cells.

In the present study, we developed targeted nanoparticles towards increased L cell stimulation to improve oral peptide delivery in incretin-based diabetes treatment. We compared the strategies in both lipid (lipid nanocapsules) and polymeric (PLGA) nanoparticles in a murine L cell line *in vitro* and in normal healthy mice *in vivo*. We also examined their antidiabetic effect *in vivo* in an obese/diabetic mouse model induced by a high-fat diet (HFD), examining the effect of the oral administration frequency.

2 Materials and methods

2.1 Materials

Exenatide (exenatide acetate) (EXE) was purchased from Bachem (Bubendorf, Switzerland). Labrafac® WL 1349 (caprylic/capric acid triglycerides) and Peceol® (oleic acid mono-, di- and triglycerides) were kindly provided by Gattefossé (Saint-Priest, France). Lipoid® S 100 (soybean lecithin at 94% of phosphatidylcholines) was a gift from Lipoid GmbH (Ludwigshafen, Germany). Solutol® HS15 (mixture of free PEG 660 and PEG 660 12-hydroxystearate, Mw 870 Da) and Span® 80 (sorbitan oleate) were purchased from Sigma-Aldrich (St. Louis, USA). The 1,2-distearoyl-sn-glycero-3-phosphoethanolamine-N-

[methoxy(polyethylene glycol)2000] (DSPE-PEG_{2000}), 1,2-distearoyl-sn-glycero-3 phosphoethanolamine-N-[polyethylene glycol)-2000]-propionate (DSPE-PEG_{2000}-CH_2-CH_2-COOH), poly(lactide-co-glycolide) (10k, d,l-LA/GA: 50:50)-block-[poly(ethylene glycol)-2000]-propionate (PLGA-PEG_{2000}-CH_2-CH_2-COOH), and poly(lactide-co-glycolide) (10k, d,l-LA/GA: 50:50)-block-[poly(ethylene glycol)-2000] methyl ether (PLGA-PEG_{2000}) were obtained from Nanosoft Polymers (Winston-Salem, USA). Lecithin, sodium chloride (NaCl), saponin, pepsin, Triton-X 100, sodium taurocholate and dimethyl sulfoxide (DMSO), 3-(4,5- dimethyl-thiazol-2-yl)-2,5-diphenyl tetrazolium bromide (MTT) were purchased from Sigma-Aldrich (St. Louis, USA). Total GLP-1 (ver.2) and active GLP-1 assay kits were purchased from Meso Scale Discovery (Maryland, USA). The Exendin-4 enzyme immunoassay kit was purchased from Phoenix Europe GmbH (Karlsruhe, Germany). the Ultrasensitive Mouse Insulin ELISA Kit was purchased from Mercodia AB (Uppsala, Sweden). Matrigel™ was obtained from BD Bioscience (Belgium). Dipeptidyl peptidase IV (DPP-IV) inhibitor was purchased from Millipore (St. Charles, USA). Dulbecco's Modified Eagle's Medium (DMEM)-GlutaMAX (5.5 Mm glucose), fetal bovine serum (FBS), penicillin-streptomycin (P/S), trypsin (0.25%)-EDTA (0.02%) and phosphate-buffered saline (PBS) were also used and purchased from Thermo Fisher Scientific (Invitrogen, Belgium). DiD (DiIC18(5) solid (1,1'-ioctadecyl-3,3,3',3'-tetramethylindodicarbocyanine,4-chlorobenzenesulfonate salt)) was obtained from Thermo Fisher Scientific (Invitrogen, UK). All chemical reagents utilized in this study were of analytical grade.

2.2 Preparation and characterization of non-targeted and targeted nanoparticles

2.2.1 Preparation of non-targeted and targeted lipid-based nanosystems—

The non-targeted lipidic nanosystem (EXE RM LNC) containing exenatide-encapsulated reverse micelles (EXE RM) and modified lipid nanocapules (LNC) was prepared as described by Xu *et al.* [11]. First, exenatide-encapsulated reverse micelles (EXE RM) were prepared by stirring under high speed a mixture consisting of Span® 80 (surfactant) and Labrafac® WL 1349 (oil) with a ratio of 1:5 wt. During stirring, 50 μL of drug solution (exenatide 30 mg/mL in MilliQ water) was dripped into the mixture. Second, LNC were produced by the phase inversion process, with slight modifications. The mixture of 769.5 mg Labrafac® WL 1349, 85.5 mg Peceol®, 13.4 mg Lipoid® S100, 120 mg Solutol® HS15, 50 mg sodium chloride (NaCl) and 1.025 mL of MilliQ water was stirred at 200 rpm for 5 min. Three progressive heating/cooling cycles (between 50 °C and 67 °C) were conducted. In the last cycle, 500 μL of pre-heated EXE RM was added to the mixture when the temperature was approximately at 3 °C above the phase inversion zone (PIZ; 59 to 61.5 °C). Finally, 2.5 mL of cold water was added to reach the PIZ temperature under high-speed stirring for 2 min. The blank non-targeted nanosystems (RM LNC) were produced using the same procedure without adding the drug solution.

2.2.2 Preparation of DiD-labeled non-targeted and targeted lipid-based nanosystems—

DiD-labeled RM LNC were prepared by adding 225 μg of DiD to the mixture. Namely, 45 μL of DiD in ethanol (5 mg/mL) was added to the vial and then heated in a water bath until the organic solvent was completely evaporated. Subsequently, Labrafac® WL 1349 was added to the same vial and mixed with DiD in the water bath until

the DiD was completely dissolved in the oil phase. The mixture was then cooled down to room temperature, other components were added and the preparation process was continued as above described.

2.2.3 Preparation of PEGylated reverse micelle-loaded lipid nanocapsules with or without propionate—PEGylated reverse micelle-loaded lipid nanocapsules with or without propionate (RM LNC PEG or RM LNC PEG-PRO, respectively) were produced by incubating DSPE-PEG_{2000} or DSPE-PEG_{2000}-CH_2-CH_2-COOH, respectively, with RM LNC at a concentration of 5 mg/mL, under gentle stirring at 37 °C for 4 h. During the incubation, the suspension was vortexed every 15 min and then quenched in an ice bath for 1 min [20].

2.2.4 Preparation of PEGylated PLGA nanoparticles with or without propionate—PLGA nanoparticles were prepared by the double emulsification method [21]. Typically, 25 mg of PLGA-PEG_{2000} or PLGA-PEG_{2000}-propionate was dissolved in 1 mL dichloromethane (DCM). For PLGA-PEG_{2000} NPs, 50 μL of an aqueous (drug) solution (in MilliQ water) was dropped into the oil phase under sonication (Digital sonifier 450, Branson, USA) at 30% amplitude for 30 s to form the primary water-in-oil emulsion. This primary emulsion was poured into 2 mL of a second aqueous phase containing 2% (w/v) saponin under sonication at 30% amplitude for 30 s to form the water-in-oil-in-water emulsion. This step was repeated twice. The emulsion was added to another 10 mL of 2% saponin solution under magnetic stirring to evaporate the organic solvent. The final nanoparticle suspension was centrifuged at 15,000 rpm for 30 min at 4 °C (Avanti® J-E centrifuge, Beckman Coulter, USA) and thoroughly washed with MilliQ water. PLGA-PEG_{2000}-PRO NPs were prepared using 1% saponin and sonication at 30% amplitude for 15 s instead.

2.2.5 Quantification of exenatide—The exenatide encapsulated within PEGylated RM LNC was quantified by high-performance liquid chromatography (HPLC, Shimadzu, Japan) using a gradient method as previously described by Xu *et al.* [11]. Briefly, a Kinetex® EVO C18 column (100 Å, 2.6 μm, 150 x 4.6 mm) (Phenomenex, USA) with a security guard column (Phenomenex, USA) was used at room temperature. The aqueous mobile phase comprised 0.05% (v/v) trifluoroacetic acid (TFA) in water, and the organic mobile phase consisted of 0.05% (v/v) in acetonitrile. A gradient system was developed with an initial ratio of 10:90 (v/v, aqueous:organic phase) at a flow rate of 1 mL/min, which was linearly changed to 90:10 (v/v) over 10 min and kept constant for the next minute. Then, the ratio was linearly changed to the initial composition in the next 1.5 min and stabilized for the last minute. The injection volume was 20 μL, and the detection wavelength was 220 nm. The retention time was 5.9 min, and the limit of detection and limit of quantification were 1.1 ± 0.4 μg/mL and 3.3 ± 1.1 μg/mL, respectively.

2.2.6 Characterization of NPs—The mean diameter and polydispersity index (PDI) of PEGylated RM LNC and PLGA NPs were determined using a Zetasizer Nano ZS (Malvern Instruments Ltd., Worcestershire, UK) by dynamic light scattering (DLS). The zeta potential was determined by Laser Doppler velocimetry (LDV) using the same device. For the

measurement, 5 μL of the nanocapsule suspension was dispersed in 995 μL of ultrapure water. All measurements were performed in triplicate.

In addition to their size, zeta potential and PDI, EXE RM LNC and PEGylated EXE RM LNC were also characterized based on their drug encapsulation efficiency (EE, %). To calculate the total drug content, 50 μL of LNC suspension were dissolved in 950 μL of methanol followed by strong vortexing. Free and encapsulated exenatide were separated by ultrafiltration using Amicon® centrifuge filters (MWCO 30 kDa, 4,000 g, 4 °C, 20 min) (Millipore). Filtrates were further diluted using a 1:2 dilution factor. The exenatide in the filtrate and the exenatide dissolved in methanol were quantified using the above-described HPLC method. The EE was calculated using the following equation:

$$\mathrm{EE}(\%) = (\text{total amount of exenatide} - \text{free exenatide})/(\text{total amount of exenatide}) \times 100$$

2.3 Nanocapsule stability and drug release in stimulated gastrointestinal fluids

2.3.1 PEGylated nanocapsule stability in stimulated gastrointestinal fluids—

The *in vitro* stability of PEGylated EXE RM LNC, with or without propionate as a ligand, was evaluated in four simulated intestinal media: Fasted State-Simulated Gastric Fluid (FaSSGF) with and without pepsin, Fasted State-Simulated Intestinal Fluid (FaSSIF) and Fed State-Simulated Intestinal Fluid (FeSSIF). The composition of these biorelevant simulated fluids has been previously described [11]. The influence of gastric and intestinal conditions on nanocapsule stability was evaluated based on the nanocapsule size and the PDI. PEGylated EXE RM LNC were incubated in the aforementioned biomimetic media at 37 °C (100 μL of nanocapsules in 10 mL of medium) under gentle stirring. At different time points (0, 0.5, 1 and 2 h for stimulated gastric media and 0, 0.5, 1, 3 and 6 h for stimulated intestinal media and FeSSIF), samples were withdrawn and analyzed by DLS.

2.3.2 *In vitro* drug release studies—

Drug release from PEGylated EXE RM LNC was evaluated in FaSSGF in the absence of pepsin and in FaSSIF media for 2 h and 6 h, respectively. Studies were performed using the dialysis method. Briefly, 1 mL of PEGylated EXE RM LNC was placed in disposable dialysis membranes (MWCO 100 kDa) (Float-A-Lyzer>G2, Microfloat, Spectrum labs, USA) and introduced into 50-mL falcon tubes containing 35 mL of medium at 37 °C under magnetic stirring. At predetermined times, 50 μL of the sample was withdrawn and dissolved in 950 μL of methanol. The concentration of exenatide was determined by HPLC as described above.

2.4 *In vitro* cell studies

2.4.1 Cell cultures—

The intestinal murine L cell line GLUTag was kindly provided by Dr. Daniel Drucker (University of Toronto, Canada). GLUTag cells were used from passages 17 to 25. Cells were grown in DMEM GlutaMAX (5.5 mM glucose) supplemented with 10% (v/v) inactivated FBS and 1% (v/v) P/S (complete DMEM medium) at 37 °C with 5% CO_2 supply. Cells were passaged every 4-5 days.

2.4.2 Cytotoxicity studies—

In vitro cytotoxicity studies of unloaded PEGylated RM LNC and PEGylated PLGA NPs were performed in GLUTag cells using nanoparticle

concentrations calculated previously using the 3-(4,5-dimethylthiazol-2-yl)-(2,5-diphenyltetrazolium bromide) (MTT) colorimetric assay [22]. GLUTag cells (5×10^4 cells per well) were seeded on Matrigel™ -coated (10 μL/mL of medium) 96-well plates. After washing the plates with prewarmed PBS buffer (x3), 100 μL of the nanoparticle suspension at increasing nanocapsule concentrations (0.5-10 mg/mL) and at increasing PLGA nanoparticle concentration (0.1-8 mg/mL) was dispersed in medium (without FBS) and co-incubated with GLUTag cells at 37 °C for 2 h. After incubation, the supernatants were replaced with 100 μL of 0.5 mg/mL MTT for 3 h. The purple formazan crystals were dissolved in 200 μL of DMSO for absorbance determination at 560 nm using a MultiSksan EX plate reader (Thermo Fisher Scientific, USA). Cells with Triton-X 100 (100% dead) and cells with culture medium (100% alive) were considered positive and negative controls, respectively. Tests were performed in triplicate.

2.4.3 *In vitro* GLP-1 secretion—

GLUTag (1.8×10^5 cells per well) were seeded onto Matrigel™-coated 24-well cell culture plates and allowed to adhere for 24 h. The next day, the plate was gently washed using prewarmed PBS. The GLUTag cells were then co-incubated with DMEM GlutaMAX without FBS or unloaded PEGylated NPs (RM LNC and PLGA NPs with or without ligand). The media contained DPP-IV inhibitor at a final concentration of 50 μM (Millipore, St. Charles, MO, USA). To test the effect of different nanoparticle concentrations on GLP-1 secretion, we used 0.5-2 mg/mL nanocapsule and 0.1-3 mg/mL nanoparticle concentrations, respectively. After 2 h of incubation at 37 °C, supernatants were collected by centrifugation (250 g, 5 min at 4 °C; Centrifuge 5804 R, Eppendorf AG, Hamburg, Germany) and preserved at –80 °C. Cells were collected in PBS containing DPP-IV inhibitor. Cell extracts containing GLP-1 were obtained after three freeze-thaw cycles followed by centrifugation at 250 g for 5 min at 4 °C. Total GLP-1 concentration was determined using a Total GLP-1 ELISA kit (Meso Scale Delivery, Gaithersburg, USA). GLP-1 secretion is expressed as the amount of GLP-1 detected in the supernatants plus cells. GLP-1 secretion was calculated using the following equation:

$$\text{GLP-1 secretion} = C_{\text{extracellular}}/(C_{\text{intracellular}} + C_{\text{extracellular}})$$

2.5 *In vivo* studies

2.5.1 Animals—

All protocols involving animal studies were approved by the Université catholique de Louvain ethical committee on animal experiments (2018/UCL/MD/45; laboratory agreement LA1230418) and conducted in accordance with the Belgian legislation regarding the protection of laboratory animals (Royal Decree of 29 May 2013).

2.5.2 Total GLP-1 secretion of ligand-conjugated and non-conjugated PEGylated NPs in normoglycemic mice—

To test PEGylated RM LNC (with or without propionate), C57BL/6J male mice (20–25 g, 10 weeks; Janvier Laboratories, France) were randomly divided into four groups (8 mice each). The animals were fasted overnight and allowed ad libitum access to water before the experiments. Mice were treated with blank RM LNC, blank PEGylated RM LNC and blank PEGylated RM LNC-PRO (~1.62 mg/g nanoparticle dose). Control mice were treated by oral gavage with an equivalent volume of MilliQ water. Blood samples were withdrawn from the tip of the tail vein at 60

and 180 min after oral administration. DPP-IV inhibitor (20 μL per mL of blood) was added to the tubes for the sample collection. The blood samples were maintained on ice and centrifuged (3,000 rpm, 10 min at 4 °C) right after the study, and the plasma was stored (-80 °C) until analysis. The total GLP-1 ELISA kit (Meso Scale Delivery, USA) was used to quantify the total GLP-1 levels.

In the case of PEGylated PLGA NPs (with or without conjugated propionate), 4 mice per group and a 200-mg/kg nanoparticle dose were used instead. The blood collection and total GLP-1 secretion analysis was conducted following the protocol described above. Total GLP-1 levels were measured under the same conditions.

2.5.3 Nanocapsule distribution in the obese/diabetic mouse small intestine and colon—Male C57BL/6J mice (8 weeks old) were randomly divided into 4 groups (n=4 per group). After acclimation (2 weeks), the mice underwent 10 weeks of HFD feeding (rodent diet with 60% fat and 20% carbohydrates (in kcal %)) (D12492i, Research Diets, USA). Before the experiments, the mice were fasted overnight with free access to water. For evaluation of the nanocapsule distribution in the small intestine and colon, DiD-labeled nanocapsules, including RM LNC, PEGylated RM LNC and PEGylated RM LNC-PRO (~1.62 mg/g nanoparticle dose), were administered orally. Control mice were orally administered an equivalent volume of MilliQ water. Sections of duodenum, jejunum, ileum and colon were excised 1 h post-administration and subsequently flash frozen in Optimal Cutting Temperature compound (OCT). For all tissues, 6-μm-thick sections were cut using a Leica CM-3050-S cryostat. The tissue sections were briefly fixed in 4% paraformaldehyde for 5 min. After washing the PBS containing 0.02% polysorbate 20, the slides were mounted with VECTASHIELD Hard Set Mounting Medium containing DAPI. The samples were examined by CLSM using a Zeiss confocal microscope (LSM 150) to capture serial images. The data were analyzed using Axio Vision software (version 4.8).

2.5.4 Mucus extraction from obese/diabetic mouse intestine—Untreated 10 week-HFD-induced diabetic mice were fasted overnight with free access to water. Prior to mucus extraction, the mice were sacrificed by cervical dislocation. The protocol followed was adapted from Wang *et al* [23]. Briefly, the duodenum and apical jejunum were dissected and placed in a Petri dish, following a very gentle flush with PBS to remove decal matter in the intestine. The syringe with a 19.5-gauge needle was used to deliver PBS gently though one open end of the intestinal segments. The intestinal segments were cut longitudinally using surgical scissors. Then, the mucus was scraped off the intestinal segments using a cell scraper (1.8 cm blade, Falcon®) and transferred to a clean tube. The isolated mucus was stored at -20 °C for further mucus diffusion and mucus stability studies.

2.5.5 Single particle tracking and confocal microcopy—DID RM LNC, DID RM LNC PEG and DID RM LNC PEG-PRO were diluted in water or small intestine mucus of mice and mixed by gentle stirring. A volume of 5 μL was placed on a microscopy glass slide sealed with an adhesive spacer (S24737, Secure-Seal™ Spacer, Thermo Fisher) and a cover glass (#1.5).

For single particle tracking, fluorescent signals were recorded using a spinning disk confocal microscope (Nikon Eclipse Ti, Tokyo, Japan) equipped with an MLC 400 B laser box (Agilent Technologies, Santa Clara, CA, USA), a Yokogawa CSU-X1 confocal spinning disk device (Andor, Belfast, UK), an iXon ultra EMCCD camera (Andor Technology, Belfast, UK) and NIS Elements software (Nikon, Japan). A 100x oil immersion objective lens (Plan Apo VC 100x oil, 1.4 NA, Nikon, Japan) was used. A stage-top incubator (37 °C, Tokai Hit) in combination with an objective lens heater (Biotechs) was used during imaging. Movies of 100 frames with a temporal resolution of 43.9 ms were recorded 5-10 μm above the coverslip. No further analysis could be performed due to either NP accumulation in distinct parts of the mucus or leakage of the fluorescent label so that individual NPs could no longer be seen or analyzed.

The samples prepared for single particle tracking were also studied by laser scanning confocal microscopy. Images were recorded on a Nikon A1R HD Confocal laser scanning microscope with a 60x/1.27 Plan Apo IR Water immersion objective (SR Plan Apo IR AC, Nikon) using a galvano scanner. A wavelength of 637 nm (LU-N4 Laser Unit) was used for excitation of DiD. Fluorescence signals were detected with a Multi-Alkali PMT (A1-DUG-2 GaAsP Multi Detector Unit). A stack of 19.5 μm above the glass surface with a step size of 0.5 μm at Nyquist resolution was recorded and a maximum intensity projection was created for visualization. All imaging was performed at RT.

2.5.6 Pharmacological studies in HFD-induced obese/diabetic mice—Male C57BL/6J mice (8 weeks old) were randomly housed (five mice per cage). After an acclimation period (2 weeks) with a normal chow diet (AIN93Mi, Research Diets, USA), the mice were fed a HFD for 10 weeks. The cages were randomly divided into 5 groups (10 mice per group) before the experiments. The mice underwent an overnight fast prior to oral gavage with free drug solution (EXE) (dose: 500 μg/kg), non-PEGylated or PEGylated drug-loaded nanosystems (EXE RM LNC or EXE RM LNC PEG) (dose: 500 μg/kg), or the empty PEGylated nanosystem (RM LNC PEG) (dose: equivalent nanocapsule concentrations to the other groups). The control HFD group was orally administered an equivalent volume of sterile water. An oral glucose tolerance test (OGTT) was performed 1 h after oral administration of the abovementioned formulations as previously described [11]. Briefly, glucose was orally administered (2 g/kg), and then blood glucose determined with a glucose meter (Accu Check, Roche, Switzerland), measuring the blood from the tip of the tail vein 30 min prior to glucose load (-30 min) and 0, 15, 30, 90 and 120 min after glucose administration. The plasma insulin and total GLP-1 levels were also tested in plasma from blood samples collected from the tail vein at -30 min and 15 min using ELISA kits (Mercodia, Uppsala, Sweden and Meso Scale Delivery, USA, respectively). The insulin resistance index was calculated by multiplying the AUC of both blood glucose and insulin during OGTT. At the end of the OGTT test, the mice were anesthetized with isoflurane (Forene, Abbott, England), and blood samples were collected from the portal vein. Active GLP-1 levels were tested by ELISA (Meso Scale Delivery, Gaithersburg, USA).

2.5.7 Pharmacokinetics study in obese/diabetic mice—Male C57BL/6J mice (8 weeks old) were housed for 2 weeks of acclimation and randomly divided into two groups

(10 mice per time point). Next, the mice underwent a HFD feeding for 10 weeks, as described in the previous section. All mice were fasted overnight with free access to sterile MilliQ water before oral gavage. Exenatide in solution and EXE RM LNC PEG were orally administered at a dose of 500 μg/kg. At predetermined time points (0, 0.5, 1, 1.5, 2, 4, 6 and 8 h), blood samples were collected from the tip of the tail vein, centrifuged (1,500 *g*, 10 min at 4 °C) and subjected to plasma extraction followed by storage at -80 °C until further analysis. Exenatide plasma concentrations were determined using ELISA kits (EK-070-94, Phoenix Europe GmbH, Karlsruhe, Germany).

2.5.8 Long-term treatment in obese/diabetic mice with different oral administration frequencies—

Male C57BL/6J mice (8 weeks old) were randomly divided into seven groups (10 mice per group) and housed at five per cage with free access to sterile food (AIN93Mi; Research Diet) (control diet) and sterile water. After 2 weeks of acclimation, the mice underwent 10 weeks of HFD or a normal control diet. After this period, the mice were treated with our formulations for an additional month, continuing with the HFD feeding (14 weeks of HFD in total). During this month, the mice were orally administered daily (D) or once every two days (T) at 4 pm (i) empty or drug-loaded PEGylated formulations (500 μg/kg dose) with daily treatment at the equivalent nanocapsule concentrations (RM LNC PEG-D or EXE RM LNC PEG-D), and (ii) non-PEGylated or PEGylated drug-loaded formulations (500 μg/kg dose) with treatment every other day (EXE RM LNC-T or EXE RM LNC PEG-T). The control groups (healthy and HFD) were orally administered an equivalent volume of sterile Milli-Q water daily. During this 4-week treatment period, the body weight of the mice was recorded daily, and glycemia was monitored once per week. Mice were fasted once per week for 6 h prior to the glucose test.

2.6 Statistical analysis

The GraphPad Prism 8 program (CA, USA) was used for the data analyses. The Grubbs test for outlier detection in each group was performed prior to all analyses. Before preforming the analysis, when there was a significant difference in the variance among groups, log-transformation was used to normalize the values. Statistical analyses were conducted using a two-way or one-way ANOVA followed by Tukey's post hoc test for studies containing more than two groups, and the *t*-test or Mann-Whitney test for two groups. The nonparametric test was conducted when there was a significant difference in variance between groups even after normalization. Statistical significance was considered at $p<0.05$. All data are expressed as the mean ± standard error of mean (SEM).

3 Results

3.1 Preparation and characterization of PEGylated nanoparticles with propionate as a targeting moiety

We first encapsulated exenatide (a GLP-1 analogue) into lipid nanocapsules (LNC) following a previously described procedure to obtain 200-nm-particle-size nanocarriers [11]. This nanoparticle size was selected based on our previous studies demonstrating the effect of lipid nanocapsules with this nanoparticle size on GLP-1 secretion [11, 22]. To develop L cell-targeted lipid-based nanocapsules, we selected DSPE-PEG_{2000} as a PEGylation linker

to provide the nanocapsules with an enhanced capacity for mucus diffusion (Fig. 1 A-B) [24]. The post-insertion method was selected to ensure the PEG chains were localized only on the surface rather than retained within the particle core. We used both DSPE-PEG_{2000}-CH_3 and DSPE-PEG_{2000}-CH_2-CH_2-COOH, the latter to provide specific targeting to L cell GPCRs present on their surface. The physicochemical properties of empty lipid nanocapsules were assessed before (RM LNC) and after the post-insertion of both DSPE-PEG_{2000}-CH_3 and DSPE-PEG_{2000}-CH_2-CH_2-COOH (RM LNC PEG and RM LNC PEG-PRO, respectively) (Fig. 1C). Blank LNC presented an ~ 200-nm particle size and a narrow size distribution (PDI=0.18). These data are in accordance with our previous results [11]. After incubation of LNC with biofunctional polymers, we observed an increase in size of ~ 18 nm and ~ 27 nm for RM LNC PEG and RM LNC PEG-PRO, respectively. The zeta potential values decreased significantly from -0.94 mV (RM LNC) to -9.93 mV (RM LNC PEG). The surface charge of RM LNC PEG-PRO decreased even more, reaching -18.20 mV in the presence of the fatty acid. We obtained a similar particle size and zeta potential after labeling the nanocarriers with DiD when compared to the respective empty nanocapsules (Fig. 1C). Additionally, there was also no significant influence on the size and surface charge of the nanocapsules when encapsulating exenatide within PEGylated nanocapsules (EXE RM LNC PEG).

To quantify the targeting capacity of propionate, we used empty PEGylated polymeric PLGA nanoparticles (PLGA NPs) with or without propionate (PLGA-PEG NPs and PLGA-PEG-PRO NPs, respectively) (Supplementary Fig. S1A). We selected these polymeric nanocarriers for this purpose because they do not trigger GLP-1 secretion by L cells when non-targeted [25]. We prepared PLGA-PEG NPs and PLGA-PEG-PRO NPs presenting a particle size of ~ 220 nm with a narrow size distribution (PDI=0.1) (Fig. S1B) to compare targeted polymeric nanoparticles with targeted lipid nanocapsules. The zeta potential of PLGA-PEG-PRO NPs decreased from -11.30 mV (PLGA-PEG NPs) to -23.50 mV after the grafting of propionate (Supplementary Fig. S1B).

3.2 (Targeted) PEGylated NPs induce GLP-1 secretion both *in vitro and in vivo*

We first investigated the ability of unloaded, PEGylated and propionate-grafted RM LNC to induce GLP-1 stimulation *in vitro* in GLUTag cells (murine L cells). We used a nanoparticle concentration ranging from 0.5 mg/mL to 2 mg/mL, after observing no evidence of cytotoxicity at concentrations below 4 mg/mL (Supplementary Fig. S2). As shown in Fig. 2A, all lipid-based formulations significantly increase endogenous GLP-1 secretion *in vitro* in L cells regardless of the nanoparticle concentration (**$p<0.05$). However, stimulation of GLP-1 secretion did not differ significantly among the tested groups, regardless of the incorporation of DSPE-PEG_{2000} or DSPE-PEG_{2000}-propionate on the surface of the nanocapsules. Thus, these strategies were not able to strengthen the nanocarrier's physiological ability to trigger GLP-1 stimulation *in vitro*. This observation of PEGylation indirectly leading to increased nanoparticle cell uptake has been reported previously [26]. To further confirm the capacity of the grafted ligand (propionate) to stimulate L cells, we also examined the L cell stimulation exerted by targeted and non-targeted PEGylated PLGA NPs. Plain PLGA NPs were found to be inert with respect to L cell stimulation [25]. Hence, if increased GLP-1 secretion was to be observed using propionate-grafted PLGA NPs, this

effect could be attributed to the ligand. PEGylated PLGA NPs failed to induce GLP-1 secretion compared with the control group for all nanoparticle concentrations tested ($p>0.05$) (Fig. 2B). The results were comparable to those observed for plain PLGA NPs [25]. Moreover, PLGA-PEG NPs grafted with propionate also did not induce GLP-1 secretion in GLUTag cells *in vitro* ($p>0.05$), further demonstrating that the introduction of propionate as a ligand on the surface of nanoparticles was not sufficient to activate the corresponding GPCRs on the surface of L cells, thus inducing GLP-1 secretion. For comparison, we also tested the GLP-1 secretion induced on murine L cells by targeting PEGylated PLGA NPs with capric acid (medium/long-chain fatty acid that binds to GPR84 (PLGA-PEG-CAP NPs)). This ligand also failed to trigger GLP-1 stimulation in murine L cells *in vitro* (Supplementary Fig. S3).

Despite the discouraging results for increased GLP-1 secretion by PEGylated lipid nanocapsules *in vitro*, and no effect of PLGA NPs, we tested whether these nanocarriers could further strengthen and/or induce GLP-1 stimulation *in vivo* in normoglycemic mice. When orally administered to normoglycemic mice, both PEGylated lipid nanocapsules (RM LNC PEG and RM LNC PEG-PRO, respectively) and non-PEGylated lipid nanocapsules (RM LNC) significantly increased GLP-1 levels 60 min post-administration ($*p<0.05$) (Fig. 2C). Notably, RM LNC PEG increased GLP-1 levels up to ~ 8-fold at 60 min, whereas RM LNC PEG-PRO had the same effect as the original unmodified RM LNC, increasing GLP-1 secretion up to ~ 4-fold compared with the untreated control group. Furthermore, only RM LNC PEG prolonged this effect at 180 min ($*p<0.05$) when compared to the control group. Although PEGylated NPs did not exert a significant effect *in vitro* when compared to non-PEGylated NPs (Fig. 2A), PEGylation could significantly improve and prolong the ability of the nanocarriers to induce GLP-1 secretion *in vivo*. However, further grafting of propionate on PEGylated RM LNC not only could not activate the GPCRs on the surface of L cells to trigger more GLP-1 secretion but also failed to achieve the same effect as PEGylated RM LNC. Moreover, when orally administering PEGylated polymeric PLGA NPs (with or without propionate), both PLGA NPs failed to increase GLP-1 secretion in normoglycemic mice (values too low to be detectable, below 0.98 pg/mL), which further confirmed that propionate decoration on the surface of the nanocarriers had no L cell-targeting effect. However, it should be taken into account that the concentration of propionate on the surface of the nanocarriers might be too low to attain the effective concentration of propionate needed to exert an effect on L cells (140 mmol/L in mice [27]). Thus, the dose of propionate within the nanocapsules could be too low to induce the desired effect.

3.3 Nanoparticle distribution in the small intestine and colon of obese/diabetic mice

We tracked the distribution of the nanocapsules in different segments of the gut after oral gavage *in vivo* in 10-week HFD-fed mice. The accumulation of DiD-labeled nanocapsules within the small intestine and the colon upon oral administration to HFD mice is depicted in Fig. 3. All the fluorescent particles (DiD RM LNC, DiD RM LNC PEG and DiD RM LNC PEG-PRO) could be found in the duodenum, in which the DiD RM LNC PEG group showed the strongest red fluorescence (DiD) compared with the other groups. RM LNC PEG-PRO seemed to fail to reach the surface of L cells and thus failed to reach the desired targeting goal when grafting fatty acids (propionate) on the surface of lipid nanocapsules.

To investigate a potential difference in mucus diffusion, we performed single particle tracking. Therefore, particles were mixed with small intestinal mucus, placed in a custom-made glass chamber and visualized on a spinning disk microscope. However, it was not possible to determine the particle diffusion *in vitro* in small intestinal mucus of mice due to a strongly reduced amount of observed particles compared with the particles in water (Supplementary Fig. S4A). With confocal microscopy, large structures with increased fluorescence intensity compared with mucus alone were observed (Supplementary Fig. S4B) for all formulations, indicating aggregation and/or binding to mucus constituents. Since the mobility of individual nanocapsules could not be investigated, it was not possible to conclude if there were any differences in net mobility between the different formulations.

DiD-labeled RM LNC were observed mainly in the duodenum and hardly in the jejunum 1 h post-administration. Interestingly, one hour after the treatment, only RM LNC PEG were able to pass through the intestinal epithelia in the jejunum, with a high level of red fluorescence observed in the epithelial basal layer (arrows) compared with the other groups. Additionally, only RM LNC PEG were able to pass through the whole small intestine (duodenum, jejunum and ileum) and reach the colon. These data could explain why PEGylated RM LNC considerably increased whereas RM LNC PEG-PRO showed no improvement of GLP-1 secretion. Complementary images on nanoparticle distribution are depicted in Supplementary Fig. S5.

3.4 Pharmacological and pharmacokinetics studies in obese/diabetic mice

As we observed no benefit of grafting propionate on the surface of PEGylated lipid nanocapsules with regard to L cell stimulation, we pursued pharmacological and pharmacokinetic studies with PEGylated nanocapsules alone. Prior to the evaluation of the efficacy of the formulation *in vivo*, we demonstrated the stability of the formulation *in vitro* in simulated gastric and intestinal fluids, and we evaluated the release profile of exenatide (Supplementary Fig. S6).

To determine the therapeutic efficacy of exenatide-loaded RM LNC PEG (EXE RM LNC PEG) on controlling the post-prandial hyperglycemia in type 2 diabetic mice, the pharmacodynamics profile was performed in 10 weeks HFD-fed mice. We administered a single dose of the nanocapsules prior to an oral glucose tolerance test (OGTT). The exenatide dose of 500 μg/kg for the free drug solution and drug-loaded formulations (including EXE in solution, EXE RM LNC and EXE RM LNC PEG, respectively), empty RM LNC PEG (equal volume as per drug-loaded nanocapsules), or an equivalent water volume was orally administered 60 min before an oral glucose challenge (glucose concentration: 2 g/kg). The time point of glucose administration corresponded to 0 h (Fig. 4A). The plasma glucose profile of drug solution-treated mice showed a similar trend as the HFD-fed mice that received water. Conversely, all the nanocapsule-treated groups, including EXE RM LNC, EXE RM LNC PEG and empty RM LNC PEG, could markedly lower blood glucose levels and the glucose area under the curve (AUC) (Fig. 4A). It is remarkable that empty RM LNC PEG had a similar efficacy for reducing plasma glucose levels and a similar AUC compared with exenatide-loaded RM LNC, indicating that the hypoglycemic effect achieved by the nanocarrier alone after PEGylation was comparable to non-PEGylated

nanocarriers encapsulating the drug. Hence, the GLP-1 levels secreted by PEGylated nanocapsules (Fig. 2C) were found to be therapeutically relevant regarding a glucose lowering effect. It is worth noting that, among all the tested formulations, only EXE RM LNC PEG orally treated mice showed significantly decreased plasma glucose levels throughout the overall OGTT test compared with untreated HFD mice.

Additionally, the total GLP-1 levels (Fig. 4B) were also significantly improved in all nanocapsule-treated groups compared with the control groups (*p<0.05). Although the increase in total GLP-1 levels in the EXE RM LNC group did not reach significant differences compared with the HFD group analyzed by the Kruskal-Wallis and Dunn's post hoc tests, significant differences were observed when the Mann-Whitney test was applied (p=0.008) (Fig. 4B). The active GLP-1 concentration measured in the portal vein (3 h post-administration of the formulation) compared with the untreated HFD mice was also significantly increased in EXE RM LNC PEG-treated mice after the OGTT test (*p<0.05) (Fig. 4C). Although there were no significant differences between the RM LNC PEG and HFD when analyzing the data by one-way ANOVA, we encountered significant differences between these groups by the Student's t-test (p=0.028). These data would confirm that PEGylation was able to improve the ability of the nanosystems to stimulate GLP-1 release and prolong this effect under pathological conditions. We encountered no differences among groups regarding insulin levels (Fig. 4D). However, EXE RM LNC PEG could dramatically reduce the insulin resistance index compared with the untreated diabetic mice (Fig. 4E). We encountered significant differences between these groups by the Student's t-test (p=0.035 and p=0.023, respectively), despite no significant differences between EXE RM LNC and RM LNC PEG by one-way ANOVA. Strikingly, we obtained a comparable result with unloaded PEGylated RM LNC when compared to EXE-loaded nanocapsules, further confirming the therapeutic relevance of the increased GLP-1 levels obtained through PEGylation.

Of note, it is our understanding that the most suitable statistical test regarding the size of our study (groups and number of animals per group) is ANOVA (parametric) or Kruskal-Wallis analysis (non-parametric). However, increasing the number of groups also increases the variability. We wanted underscore that the large number of groups and the variability of the study could have hindered the identification of more significant differences among the groups. We used the appropriate statistical test in the figure, but we wanted to highlight the differences encountered among groups, pointing to a strong physiological effect, as shown by the differences encountered when conducting the Student's t-test or Mann-Whitney test (parametric and non-parametric tests comparing two groups only).

To investigate the oral delivery of exenatide via PEGylated RM LNC, a pharmacokinetic study was performed to evaluate the oral absorption of exenatide in chronic diabetic mice (10 weeks of HFD; n=10 per point) after oral administration of a single dose of 500 μg/kg exenatide via drug solution or within RM LNC PEG (EXE RM LNC PEG) (Fig. 4F). A different pattern of exenatide absorption was observed in obese/diabetic mice after oral gavage of drug solution alone or EXE RM LNC PEG. When orally administered as a solution, the plasma concentration of exenatide remained unchanged throughout the testing period. In comparison, EXE RM LNC PEG elicited greater systemic absorption of the

peptide after oral administration for 8 h, with a T_{max} and C_{max} of 1 h and 27.91 ± 1.22 ng/mL, respectively. Supplementary Table S1 summarizes the calculated parameters obtained in this pharmacokinetic study. One should note that a different exenatide pharmacokinetic profile (e.g., different C_{max}, AUC, T_{max}) was observed after oral administration of EXE RM LNC PEG versus EXE RM LNC [11], indicating that PEGylation extended the circulation time of the formulation ($t_{1/2}$ of the drug-loaded formulation prolonged from 1.68 ± 0.35 to 5.69 ± 1.02 h) and then increased the systemic absorption of the encapsulated peptide (AUC increased from 11.79 ± 2.73 to 27.91 ± 1.22 $ng \cdot mL^{-1} \cdot min^{-1}$).

3.5 Long-term treatment with PEGylated lipid nanocapsules in obese/diabetic mice

To investigate the impact of the increased GLP-1 secretion observed after PEGylation on glucose metabolism, we performed a long-term treatment (one month) in diabetic mice (10 weeks HFD), administering exenatide-loaded or unloaded RM LNC PEG (500 μg/kg) with different administration frequencies (daily or once every other day) (14 weeks of HFD in total, daily or every other day administrations for 4 weeks from week 10). The mice treated less frequently by oral administration (once every other day) (EXE RM LNC PEG; 500 μg/kg), or with identical amounts of unloaded PEGylated nanocapsules (RM LNC PEG), were also compared with those that received non-PEGylated EXE-loaded nanocapsules (EXE RM LNC; 500 μg/kg) following the administration regimen.

The plasma glucose levels were monitored weekly during the 4 weeks of treatment and are depicted in Supplementary Fig. S7. The plasma glucose and insulin levels and the calculated HOMA-IR after a 4 weeks of treatment are depicted in Fig. 5. The PEGylated groups (loaded or unloaded) administered on a daily basis and the EXE-loaded PEGylated group administered every other day exhibited comparable glucose plasma levels. These levels were in turn comparable to the non-obese/diabetic untreated control mice ($p>0.05$, Fig. 5A). It is noteworthy that only when PEGylated nanocapsules were encapsulating EXE were effective for lowering glucose plasma levels following a long-term treatment. More importantly, they were efficient even with less frequent administration, which was the main goal of the present study (Fig. 5A). Additionally, these groups exhibited equivalent insulin resistance, as analyzed by homeostatic model assessment of insulin resistance (HOMA-IR), which were comparable to the control values obtained for the healthy control group ($p>0.05$) (Fig. 5C). Compared with the HFD group, the reduction among these groups was not statistically significant using the Kruskal-Wallis followed by Dunn's post hoc test (Fig. 5C). However, significant differences were observed when the Mann-Whitney test was used ($p=0.0012$ for EXE RM LNC PEG-D versus HFD, $p=0.0003$ for RM LNC PEG-D treatment versus HFD, and $p=0.05$ for EXE RM LNC PEG-T treatment versus HFD, respectively).

4 Discussion

The aim of the present study was to increase the L cell stimulation exerted by our nanocarriers, thus increasing the induced secreted GLP-1 levels. This would allow us to prolong the *in vivo* antidiabetic effect exerted by our nanosystem towards less frequent peptide administrations. To achieve this goal, the aim of this study was to develop targeted-

nanosystems towards increased L cell stimulation. Based on the literature [29], we chose propionate as the fatty acid for grafting on the surface of our lipid-based nanocapsules, as it is known to be a potent highly effective ligand for GPCRs located on the surface of L cells.

We first evaluated the ability of propionate-targeted lipid-based formulations to stimulate GLP-1 secretion by L cells *in vitro* in murine GLUTag cells. All tested lipid-based nanocarriers effectively increased the secretion of GLP-1 by L cells, regardless of being grafted with propionate (Fig. 2A). Indeed, grafting the surface of lipid nanocapsules with propionate did not provide any additional advantage compared with plain nanocapsules. However, as we pointed out, the propionate dose administered within the nanocapsules might be insufficient to induce an effect. The same results were observed when PLGA-based nanoparticles were grafted with both propionic and capric acid (Fig. 2B). As PLGA nanoparticles failed to increase GLP-1 *in vitro*, we tested the effect of lipid-based nanocapsules (propionate-targeted or not) *in vivo* in normoglycemic mice. Surprisingly, we found out that RM LNC with PEG alone (the linker used to graft propionate on the surface of LNC) (RM LNC PEG) significantly increased secreted GLP-1 levels from ~ 4-fold to ~ 8-fold at 60 min, prolonging the effect observed for RM LNC and increasing the effect at least up to 180 min (Fig 2C). Propionate-grafted nanocapsules (RM LNC PEG-PRO) significantly increased GLP-1 secretion compared with the control untreated group at 60 min. However, the effect was significantly lower than the effect exerted by PEGylated lipid nanocapsules alone and was not prolonged (p>0.05 at 180 min) (Fig. 2C). We further investigated the localization of nanocapsules (fluorescence) in 10-week HFD-treated obese/diabetic mice 1 h after oral gavage of the formulation (Fig. 3). We chose to evaluate the effect directly in a diabetic model and not in normoglycemic mice because the number of L cells is known to be increased in the pathological context [30]. After 1 h of treatment, DiD-RM LNC PEG showed the strongest red fluorescence (DiD) in the intestinal lumen, and they were able to pass through the whole small intestine (duodenum, jejunum and ileum) to finally reach the colon. It should be noted that the colon harbors the highest amount of enteroendocrine L cells in the entire gut [31].

The ultimate goal of our study was to prolong the *in vivo* antidiabetic effect exerted by our nanosystem towards less frequent peptide administrations. For this purpose, once confirmed propionate-targeted nanoparticles were not exerting the desired effect, we pursued studies with PEGylated lipid nanocapsules. We evaluated the ability of PEGylated nanocapsules and their non-PEGylated counterparts, EXE-loaded or unloaded, to improve glycemia *in vivo* in obese/diabetic mice (10 weeks of HFD feeding) following acute or chronic treatment. For the acute treatment with a single dose, all tested nanoparticles, PEGylated or not, were able to normalize blood glucose levels, significantly increasing GLP-1 secretion. However, only PEGylated nanoparticles were able to significantly increase active GLP-1 secretion, and the secreted circulating GLP-1 levels were higher than those observed for the non-PEGylated nanoparticles. We observed a different exenatide pharmacokinetic profile for EXE RM LNC PEG compared with our previous studies with EXE RM LNC [9]. The PEGylation extended the circulation time of the formulation ($t_{1/2}$ of the drug-loaded formulation prolonged from 1.7 ± 0.4 to 5.7 ± 1.0 h) and then increased the systemic absorption of the encapsulated peptide (AUC increased from 11.8 ± 2.7 to 27.9 ± 1.2 ng·mL^{-1}·min-1).

To further demonstrate that the PEGylated nanosystem could efficiently prolong the *in vivo* antidiabetic effect and help minimize the administration frequency, we performed a chronic/long-term therapy consisting of a 4 weeks of treatment with a protocol including two different administration regimens: once daily (D) or once every other day (T). After a 4-week treatment, EXE RM LNC PEG-T (administered once every other day), RM LNC PEG-D and EXE RM LNC PEG-D (administered daily) mice showed normalized plasma glucose levels (Fig. 5A), which significantly reduced insulin resistance (measured by HOMA-IR, Fig. 5C). We were thus able to obtain comparable results among PEGylated nanocapsules, reaching basal glucose levels even with less frequent administration when encapsulating EXE. Interestingly, when administered once daily, the unloaded PEGylated nanocapsules were also able to reach basal glucose levels and significantly reduce insulin resistance, confirming that the increase in GLP-1 secretion (~8-fold) was a sufficient stimulus for lowering glucose levels. Moreover, this effect was prolonged over time, allowing us to reduce the administration frequency.

5 Conclusion

In conclusion, we reached our goal of increasing GLP-1 secretion and prolonging the antidiabetic effect of our formulation via PEGylation. Although many questions remain (e.g. the exact mechanism of action, potential toxicity to the gastrointestinal tract following frequent administrations, anti-PEG antibodies in the clinic), we have demonstrated our proof-of-concept that we can decorate the surface of our nanocapsules to modulate their effect on GLP-1 secretion. This finding brings hope for the treatment not only of type 2 diabetes mellitus but also other gastrointestinal diseases that require the secretion of other gastrointestinal peptides (e.g., inflammatory bowel diseases), as well as the use of nanomedicine for oral peptide delivery. All these developments will help foster the translation of this approach to the clinics

Supplementary Material

Refer to Web version on PubMed Central for supplementary material.

Acknowledgments

YX is a PhD student supported by a grant from the China Scholarship Council (CSC). AB is a research associate from the Belgian FRS-FNRS (Fonds de la Recherche Scientifique). PDC is senior research associate from the Belgian FRS-FNRS under grants WELBIO-CR-2019C-02R and The Excellence Of Science (EOS 30770923) and is a recipient of the Funds Baillet Latour (Grant for Medical Research 2015). This work was supported by the FRS-FNRS (convention T.0013.19). This project has received funding from the European Research Council (ERC) under the European Union's Horizon 2020 research and innovation programme (grant agreement No. 850997).

Data availability

All data relevant to the study are included in the article or uploaded as supplementary information. Complementary data that support the findings of this study are available from the corresponding author, AB, upon reasonable request.

Europe PMC Funders Author Manuscripts

References

[1]. Fosgerau K, Hoffmann T. Peptide therapeutics: current status and future directions. Drug Discov Today. 2015; 20(1):122–8. [PubMed: 25450771]

[2]. Richard J. Challenges in oral peptide delivery: lessons learnt from the clinic and future prospects. Ther Deliv. 2017; 8(8):663–684. [PubMed: 28730934]

[3]. Tyagi P, Pechenov S, Subramony J Anand. Oral peptide delivery: Translational challenges due to physiological effects. J Control Release. 2018; 287:167–176. [PubMed: 30145135]

[4]. Niu Z, Conejos-Sanchez I, Griffin BT, O'Driscoll CM, Alonso MJ. Lipid-based nanocarriers for oral peptide delivery. Adv Drug Deliv Rev. 2016; 106(Pt B):337–354. [PubMed: 27080735]

[5]. Aguirre TA, Teijeiro-Osorio D, Rosa M, Coulter IS, Alonso MJ, Brayden DJ. Current status of selected oral peptide technologies in advanced preclinical development and in clinical trials. Adv Drug Deliv Rev. 2016; 106(Pt B):223–241. [PubMed: 26921819]

[6]. Kim LS, Hadley WK, Stansell J, Cello JP, Koch J. Declining prevalence of cryptosporidiosis in San Francisco. Clin Infect Dis. 1998; 27(3):655–6. [PubMed: 9770178]

[7]. Qualmann C, Nauck MA, Holst JJ, Orskov C, Creutzfeldt W. Insulinotropic actions of intravenous glucagon-like peptide-1 (GLP-1) [7-36 amide] in the fasting state in healthy subjects. Acta Diabetol. 1995; 32(1):13–6. [PubMed: 7612912]

[8]. Bouttefeux O, Beloqui A, Preat V. Delivery of Peptides Via the Oral Route: Diabetes Treatment by Peptide-Loaded Nanoparticles. Curr Pharm Des. 2016; 22(9):1161–76. [PubMed: 26675223]

[9]. Brayden DJ, Alonso MJ. Oral delivery of peptides: opportunities and issues for translation. Adv Drug Deliv Rev. 2016; 106(Pt B):193–195. [PubMed: 27865345]

[10]. Drucker DJ. Advances in oral peptide therapeutics. Nat Rev Drug Discov. 2019

[11]. Xu Y, Van Hul M, Suriano F, Preat V, Cani PD, Beloqui A. Novel strategy for oral peptide delivery in incretin-based diabetes treatment. Gut. 2019

[12]. Li C, Zhao Y, Cheng J, Guo J, Zhang Q, Zhang X, Ren J, Wang F, Huang J, Hu H, Wang R, et al. A Proresolving Peptide Nanotherapy for Site-Specific Treatment of Inflammatory Bowel Disease by Regulating Proinflammatory Microenvironment and Gut Microbiota. Adv Sci (Weinh). 2019; 6(18)

[13]. Martins JP, Liu D, Fontana F, Ferreira MPA, Correia A, Valentino S, Kemell M, Moslova K, Makila E, Salonen J, Hirvonen J, et al. Microfluidic Nanoassembly of Bioengineered Chitosan-Modified FcRn-Targeted Porous Silicon Nanoparticles @ Hypromellose Acetate Succinate for Oral Delivery of Antidiabetic Peptides. ACS Appl Mater Interfaces. 2018; 10(51):44354–44367. [PubMed: 30525379]

[14]. Lakkireddy HR, Bazile D. Building the design, translation and development principles of polymeric nanomedicines using the case of clinically advanced poly(lactide(glycolide))-poly(ethylene glycol) nanotechnology as a model: An industrial viewpoint. Adv Drug Deliv Rev. 2016; 107:289–332. [PubMed: 27593265]

[15]. des Rieux A, Pourcelle V, Cani PD, Marchand-Brynaert J, Preat V. Targeted nanoparticles with novel non-peptidic ligands for oral delivery. Adv Drug Deliv Rev. 2013; 65(6):833–44. [PubMed: 23454185]

[16]. Chimerel C, Emery E, Summers DK, Keyser U, Gribble FM, Reimann F. Bacterial metabolite indole modulates incretin secretion from intestinal enteroendocrine L cells. Cell Rep. 2014; 9(4):1202–8. [PubMed: 25456122]

[17]. Brown AJ, Goldsworthy SM, Barnes AA, Eilert MM, Tcheang L, Daniels D, Muir AI, Wigglesworth MJ, Kinghorn I, Fraser NJ, Pike NB, et al. The Orphan G protein-coupled receptors GPR41 and GPR43 are activated by propionate and other short chain carboxylic acids. J Biol Chem. 2003; 278(13):11312–9. [PubMed: 12496283]

[18]. Le Poul E, Loison C, Struyf S, Springael JY, Lannoy V, Decobecq ME, Brezillon S, Dupriez V, Vassart G, Van Damme J, Parmentier M, et al. Functional characterization of human receptors for short chain fatty acids and their role in polymorphonuclear cell activation. J Biol Chem. 2003; 278(28):25481–9. [PubMed: 12711604]

[19]. Morrison DJ, Mackay WG, Edwards CA, Preston T, Dodson B, Weaver LT. Butyrate production from oligofructose fermentation by the human faecal flora: what is the contribution of extracellular acetate and lactate? Br J Nutr. 2006; 96(3):570–7. [PubMed: 16925864]

[20]. Perrier T, Saulnier P, Fouchet F, Lautram N, Benoit JP. Post-insertion into Lipid NanoCapsules (LNCs): From experimental aspects to mechanisms. Int J Pharm. 2010; 396(1-2):204–9. [PubMed: 20600733]

[21]. Xu Q, Boylan NJ, Cai S, Miao B, Patel H, Hanes J. Scalable method to produce biodegradable nanoparticles that rapidly penetrate human mucus. J Control Release. 2013; 170(2):279–86. [PubMed: 23751567]

[22]. Xu Y, Carradori D, Alhouayek M, Muccioli GG, Cani PD, Preat V, Beloqui A. Size Effect on Lipid Nanocapsule-Mediated GLP-1 Secretion from Enteroendocrine L Cells. Mol Pharm. 2018; 15(1):108–115. [PubMed: 29226685]

[23]. Wang R, Hasnain SZ. Analyzing the Properties of Murine Intestinal Mucins by Electrophoresis and Histology. Bio-protocol. 2017; 7(14):e2394.

[24]. Huckaby JT, Lai SK. PEGylation for enhancing nanoparticle diffusion in mucus. Adv Drug Deliv Rev. 2018; 124:125–139. [PubMed: 28882703]

[25]. Beloqui A, Alhouayek M, Carradori D, Vanvarenberg K, Muccioli GG, Cani PD, Preat V. A Mechanistic Study on Nanoparticle-Mediated Glucagon-Like Peptide-1 (GLP-1) Secretion from Enteroendocrine L Cells. Mol Pharm. 2016; 13(12):4222–4230. [PubMed: 27934480]

[26]. Pelaz B, del Pino P, Maffre P, Hartmann R, Gallego M, Rivera-Fernandez S, de la Fuente JM, Nienhaus GU, Parak WJ. Surface Functionalization of Nanoparticles with Polyethylene Glycol: Effects on Protein Adsorption and Cellular Uptake. ACS Nano. 2015; 9(7):6996–7008. [PubMed: 26079146]

[27]. Tolhurst G, Heffron H, Lam YS, Parker HE, Habib AM, Diakogiannaki E, Cameron J, Grosse J, Reimann F, Gribble FM. Short-chain fatty acids stimulate glucagon-like peptide-1 secretion via the G-protein-coupled receptor FFAR2. Diabetes. 2012; 61(2):364–71. [PubMed: 22190648]

[28]. Amrutkar M, Cansby E, Chursa U, Nunez-Duran E, Chanclon B, Stahlman M, Friden V, Manneras-Holm L, Wickman A, Smith U, Backhed F, et al. Genetic Disruption of Protein Kinase STK25 Ameliorates Metabolic Defects in a Diet-Induced Type 2 Diabetes Model. Diabetes. 2015; 64(8):2791–804. [PubMed: 25845663]

[29]. Tirosh A, Calay ES, Tuncman G, Claiborn KC, Inouye KE, Eguchi K, Alcala M, Rathaus M, Hollander KS, Ron I, Livne R, et al. The short-chain fatty acid propionate increases glucagon and FABP4 production, impairing insulin action in mice and humans. Sci Transl Med. 2019; 11(489)

[30]. Kappe C, Zhang Q, Nystrom T, Sjoholm A. Effects of high-fat diet and the anti-diabetic drug metformin on circulating GLP-1 and the relative number of intestinal L-cells. Diabetol Metab Syndr. 2014; 6:70. [PubMed: 25028601]

[31]. Bodnaruc AM, Prud'homme D, Blanchet R, Giroux I. Nutritional modulation of endogenous glucagon-like peptide-1 secretion: a review. Nutr Metab (Lond). 2016; 13:92. [PubMed: 27990172]

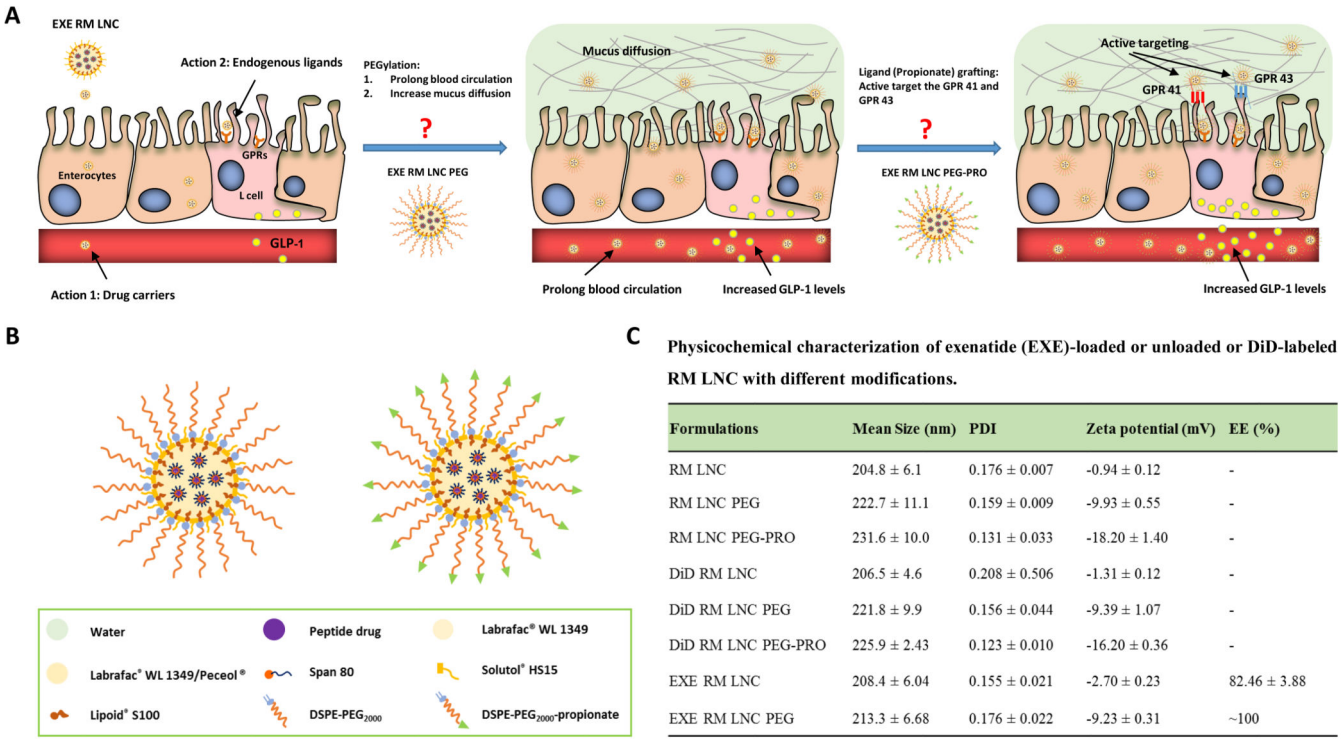

C

Physicochemical characterization of exenatide (EXE)-loaded or unloaded or DiD-labeled RM LNC with different modifications.

Formulations	Mean Size (nm)	PDI	Zeta potential (mV)	EE (%)
RM LNC	204.8 ± 6.1	0.176 ± 0.007	-0.94 ± 0.12	-
RM LNC PEG	222.7 ± 11.1	0.159 ± 0.009	-9.93 ± 0.55	-
RM LNC PEG-PRO	231.6 ± 10.0	0.131 ± 0.033	-18.20 ± 1.40	-
DiD RM LNC	206.5 ± 4.6	0.208 ± 0.506	-1.31 ± 0.12	-
DiD RM LNC PEG	221.8 ± 9.9	0.156 ± 0.044	-9.39 ± 1.07	-
DiD RM LNC PEG-PRO	225.9 ± 2.43	0.123 ± 0.010	-16.20 ± 0.36	-
EXE RM LNC	208.4 ± 6.04	0.155 ± 0.021	-2.70 ± 0.23	82.46 ± 3.88
EXE RM LNC PEG	213.3 ± 6.68	0.176 ± 0.022	-9.23 ± 0.31	~100

Figure 1.

Targeting strategies towards increased L cell stimulation to achieve increased endogenous GLP-1 secretion. (A) Graphic description of the two steps used to prepare L cell-targeted nanocarriers. Step one: provision of the nanosystem with stealth properties (PEGylation) aimed at (i) increasing the mucopenetration, (ii) thus further enhancing GLP-1 secretion by increasing the number of nanocarriers able to gain access to L cells and ultimately (iii) prolonging the blood circulation of the nanosystems upon intestinal absorption. Step two: grafting of propionate on the surface of the nanosystems to improve L cell active targeting and to strengthen the GLP-1 secretory effect. (B) Schematic representation of exenatide-loaded RM LNC PEG and RM LNC PEG-PRO. (C) Physicochemical characterization of empty, DiD-labeled or exenatide-loaded RM LNC after including the different surface modifications (mean ± SEM; n=9). For the schematic representation of EXE RM LNC please refer to [11].

Europe PMC Funders Author Manuscripts

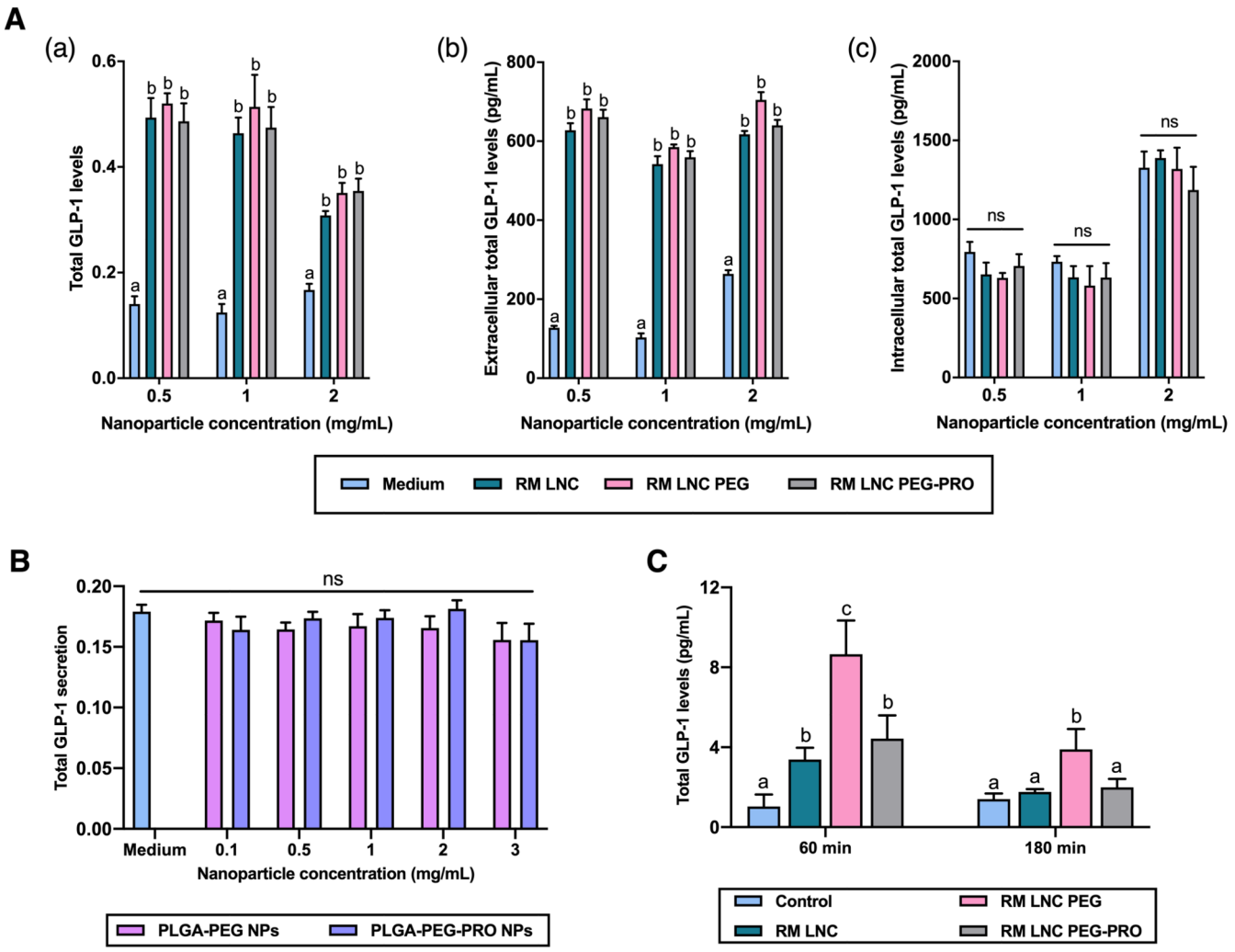

Figure 2.

Effect of PEGylated NPs (with or without propionate grafted as a ligand) on GLP-1 stimulation in GLUTag cells (murine L cells) and in normoglycemic mice. (A) Effect of PEGylated RM LNC (with or without propionate grafted as a ligand) on GLP-1 stimulation in murine GLUTag cells after 2 h of co-incubation with increasing nanocapsule concentrations from 0.5 to 2 mg/mL (mean ± SEM; n=4; N=3). (B) Effect of polymeric PLGA-PEG NPs (with or without propionate grafted as a ligand) on GLP-1 secretion from GLUTag cells after 2 h of co-incubation with an increasing nanoparticle concentration from 0.1 to 3 mg/mL (mean ± SEM; n=4; N=3). (C) Total GLP-1 levels in healthy control mice 60 and 180 min post-oral gavage with RM LNC, RM LNC PEG and RM LNC PEG-PRO using the same nanocapsule dose (1.62 mg/g) (mean ± SEM; n=8). Different superscript letters represent significant differences between the groups (*p<0.05) based on two-way analysis of variance followed by Tukey's post hoc test (A), the Mann-Whitney test (B) or one-way ANOVA followed by Tukey's post hoc test (C).

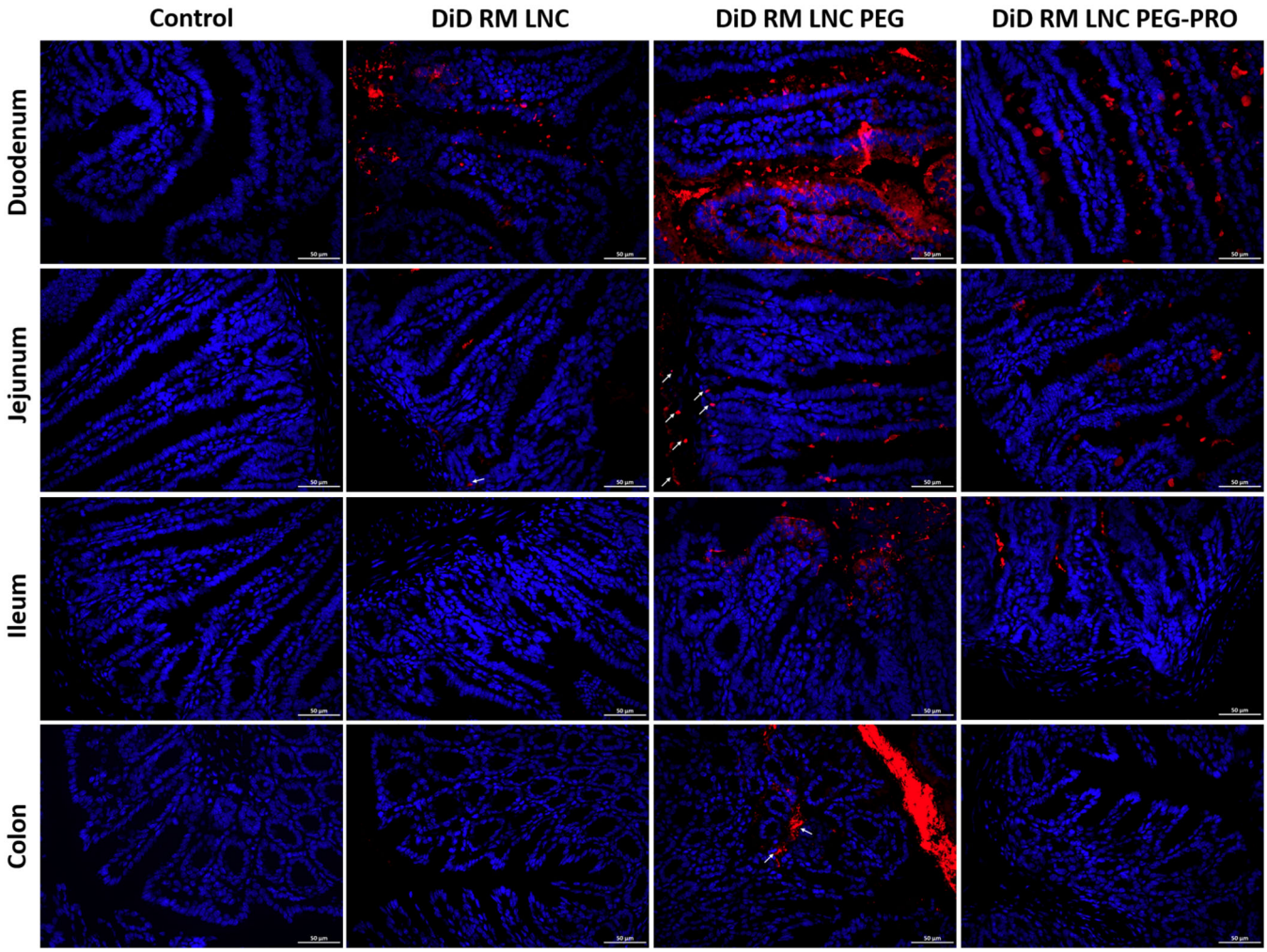

Figure 3.

In vivo distribution within the small intestine and the colon of mice. Representative images of the fluorescent nanocapsule (red) distribution in the duodenum, jejunum, ileum and colon in 10-week HFD obese/diabetic mice 1 h after the oral gavage of MilliQ water, DiD RM LNC, DiD RM LNC PEG and DiD RM LNC PEG-PRO (1.62 mg/g nanoparticle dose) (n = 4). The images show merged fluorescent nanocapsules (red)/DAPI (blue) staining of the cell nucleus. White arrows point to lipid-based nanocapsules. Scale bar = 50 μm.

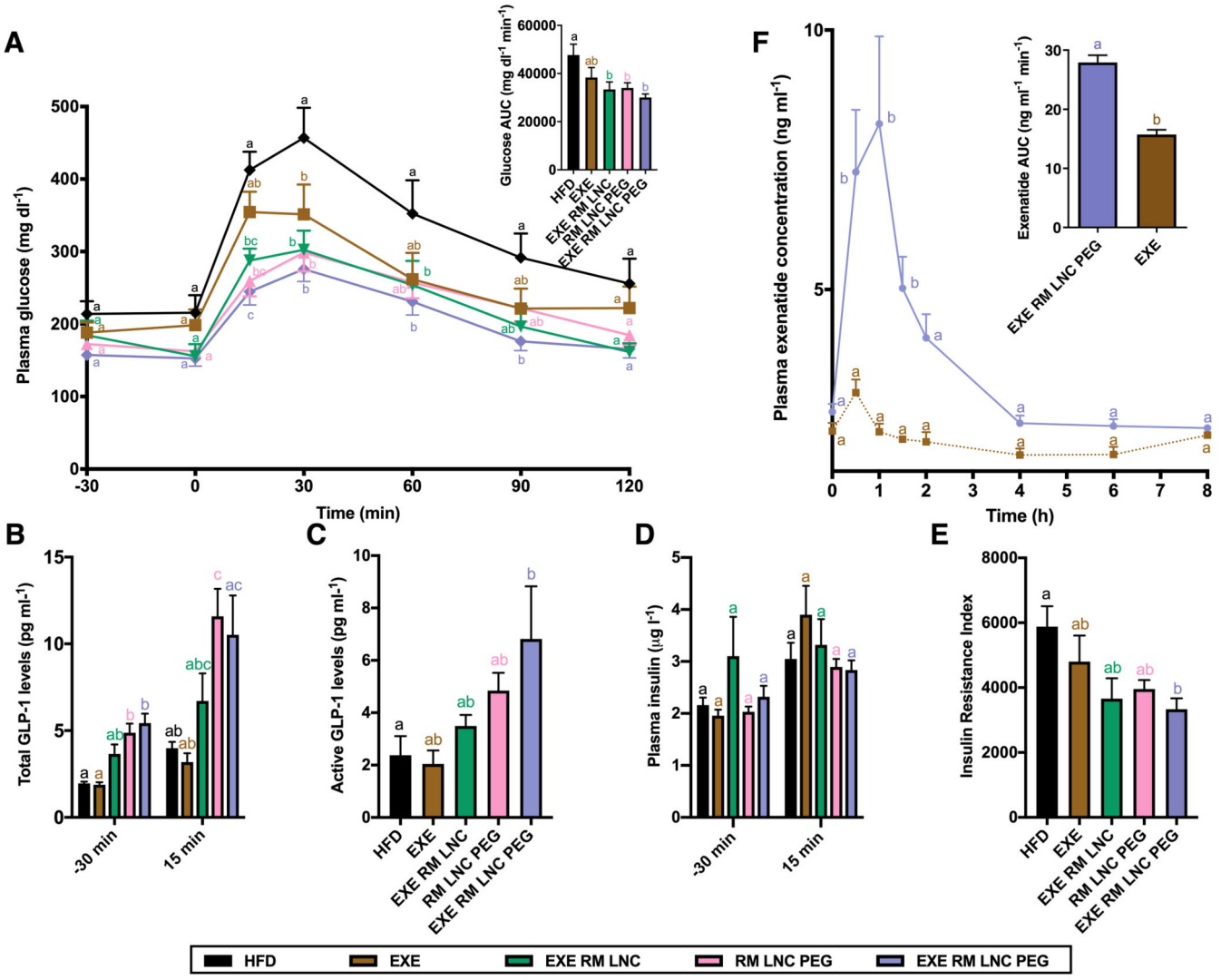

Figure 4.

Pharmacological and pharmacokinetics studies in obese/diabetic mice after a single orally administered dose. (A) Blood glucose values (mg·dL^{-1}) and mean AUC (mg·dL·min^{-1}) were tested 30 min before and 120 min after glucose administration (n=7–8). (B) Plasma total GLP-1 concentrations were measured 30 min before and 15 min after glucose administration (n=6–8). (C) Active GLP-1 levels measured in the portal vein of obese/diabetic mouse after OGTT (3 h post-administration of the formulation) (n=6–8). (D) Insulin concentrations were measured in plasma collected from blood from the tail vein 30 min before and 15 min after oral glucose administration (n=6–8). (E) Insulin resistance index (n=7–8). (F) Plasma exenatide concentration-time profile and exenatide AUC in diabetic mice (10 weeks of HFD feeding) after oral administration of the drug solution or drug-loaded PEGylated nanocapsules (EXE and EXE RM LNC PEG, respectively) (dose: 500 μg/kg) (n=9-10). Data are shown as the mean ± SEM. Different superscript letters indicate a significant difference among the groups (*p<0.05) by two-way analysis of variance (ANOVA) and Tukey's post

Europe PMC Funders Author Manuscripts

hoc test (A, F), the Kruskal-Wallis followed by Dunn's post hoc test (B) or one-way ANOVA followed by Tukey's post hoc test (C-E).

Europe PMC Funders Author Manuscripts

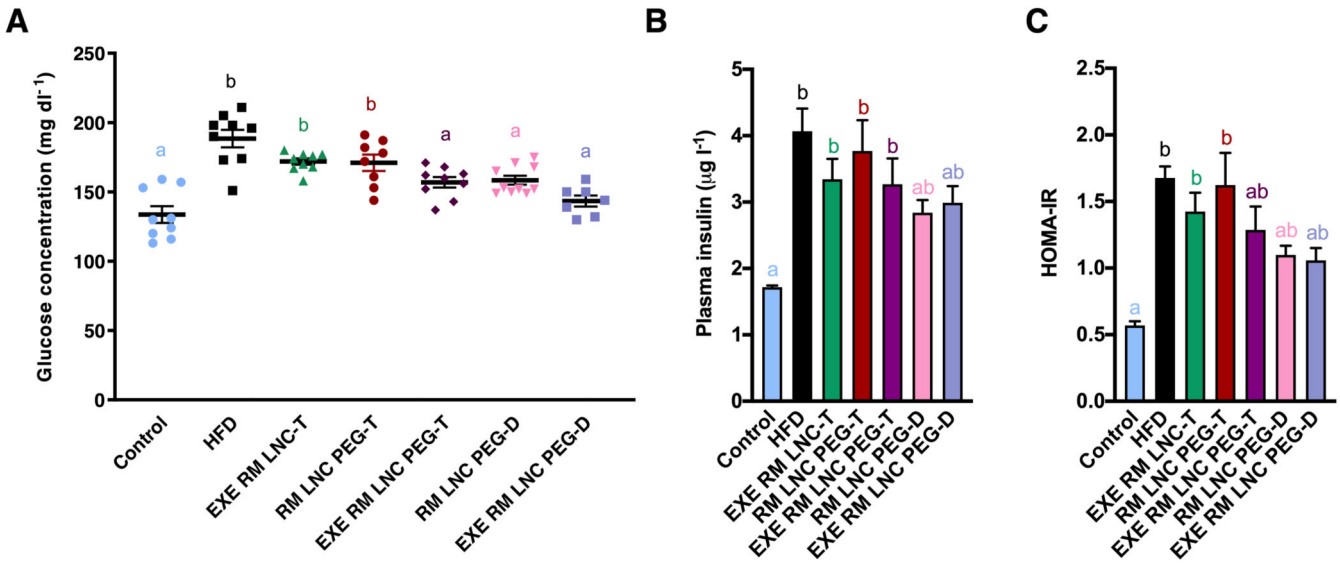

Figure 5.

Effect of PEGylated and non-PEGylated EXE-loaded lipid nanocapsules with different oral administration frequencies on the suppression of hyperglycemia and hyperinsulinemia in HFD diet-induced diabetic mice via long-term therapy. (A) Plasma glucose values (mg(dL^{-1}) after 4 weeks of administration (HFD feeding for 14 weeks in total) (mean ± SEM; n=7-10). (B) Insulin concentrations were tested in the plasma from blood retrieved from the tail vein (mean ± SEM; n=6-9). (C) HOMA-IR was calculated using the equation [fasting glucose in mg/dL × fasting insulin in ng/mL]/405 as previously defined [28] (mean ± SEM; n=8-9). Different superscript letters show statistically significant differences among the groups (*$p<0.05$) based on two-way analysis of variance followed by Tukey's post hoc test (A), or the Kruskal-Wallis followed by Dunn's post hoc test (B, C).

Europe PMC Funders Author Manuscripts